

Bias dependent dual band response from InAs/Ga(In)Sb type II strain layer superlattice detectors

A. Khoshakhlagh, J. B. Rodriguez, E. Plis, G. D. Bishop, Y. D. Sharma, H. S. Kim, L. R. Dawson, and S. Krishna^{a)}

Center for High Technology Materials, Department of Electrical and Computer Engineering, University of New Mexico, Albuquerque, New Mexico 87106, USA

(Received 10 October 2007; accepted 23 November 2007; published online 27 December 2007)

We report on the multispectral properties of infrared photodetectors based on type II InAs/Ga(In)Sb strain layer superlattices using an nBn heterostructure design. The optical and electrical properties of the midwave and long wave infrared (MWIR-LWIR) absorbing layers are characterized using spectral response and current-voltage measurements, respectively. The dual band response is achieved by changing the polarity of applied bias. The spectral response shows a significant change in the LWIR to MWIR ratio within a very small bias range (~ 100 mV), making it compatible with commercially available readout integrated circuits. © 2007 American Institute of Physics.

[DOI: 10.1063/1.2824819]

Infrared (IR) photodetectors are useful for a variety of military and civil applications, such as target acquisition, medical diagnostics, and pollution monitoring, to name just a few. Presently, photonic IR detectors are based on interband transitions in low bandgap semiconductors, such as mercury cadmium telluride (MCT) or InSb, or in intersubband transitions in heteroengineered structures, such as quantum well or quantum dot infrared photodetectors (QWIPs or QDIPs).^{1,2} In the past few years, interband transitions in type II InAs/GaSb strain layer superlattices (SLS) have emerged as a competing technology. Although MCT and QWIP technologies are relatively more mature than the SLS technology, the SLS technology has potential to enhance performance in several key areas. Detectors based on InAs/GaSb superlattices have already shown promising results in operating at higher temperature.³ However, most of the present day SLS photodetectors are based on photodiode (*p-i-n*) design.^{4,5} The lack of a stable passivation layer for the etched mesa surface for the SLS photodiodes is one of the primary limitations of the SLS based technology.

A class of IR detectors named nBn has recently shown promising results in eliminating the currents associated with Shockley-Read-Hall centers and mesa lateral surface imperfections, which have resulted in an increase of the operating temperature⁶ as compared to the *p-i-n* design. This nBn IR detector has demonstrated a 100 K increase in the background limited temperature (BLIP) with an InAs bulk active region. Our research group recently reported a SLS based nBn structure with cutoff wavelength equal to $5.2 \mu\text{m}$ with quantum efficiency, and a shot noise limited specific detectivity D^* comparable to the state of art midwave infrared (MWIR) *p-i-n* diodes based on the same material.⁷

We are presently investigating the multispectral detection capabilities of type II InAs/Ga(In)Sb SLS detector based on an nBn design. Multicolor detectors are desirable in a variety of IR applications related to remote sensing and object identification. Dual band, MWIR, and long wave infrared (LWIR) also have interesting applications such as

computed-tomography imaging spectrometer.⁸ Multicolor capabilities have been demonstrated with MCT and QWIP and more recently in the SLS system.⁹ Present day two color SLS detector requires two contacts per pixel leading to a complicated processing scheme and expensive specific readout circuits (ROICs). In this letter, we present a bias dependent dual band SLS detector operating in the MWIR and LWIR regions. One of the advantages of this design is that it is compatible with the standard single bump per contact processing, which reduces the cost and complexity associated with the fabrication process.

To study the devices with type II InAs/(In)GaSb SLS absorbers based on nBn design, we grew two samples, referred to as structures A and B. Structures A and B consist of MWIR and LWIR absorber layers, shown as insets in Figs. 1(a) and 1(b), respectively. Spectral measurements were performed on structures A and B at temperatures ranging from 50 to 300 K using a Nicolet 670 Fourier transform infrared spectrometer and a Keithley 428 preamplifier. The relative spectral response was obtained by dividing the photocurrent of the $300\text{-}\mu\text{m}$ -diameter aperture nBn SLS detectors with that obtained using a calibrated¹⁰ deuterated triglycine sulfate thermal detector. Two color responses ($\lambda_{c1} \sim 3.5 \mu\text{m}$ and $\lambda_{c2} \sim 4.5 \mu\text{m}$) and ($\lambda_{c1} \sim 3.5 \mu\text{m}$ and $\lambda_{c2} \sim 8 \mu\text{m}$) were seen at different polarities of applied bias. The relative spectral responses of structures A and B at 100 and 150 K as a function of applied voltage bias are displayed in Figs. 1(a) and 1(b), respectively. These show clear two color response under different polarity. We believe that the two responses come from the SLS absorber and the SLS contact layer.

Figure 2 shows the conduction band profile of structures A and B under forward and reverse biases. Under forward bias [Fig. 2(a)], the photocarriers from the absorber are collected. When the device is under reverse bias [Fig. 2(b)], the photocarriers from the heavily *n*-doped top contact layer are collected and the photocarriers from the absorber are blocked by the barrier. Heavily doped InAs in the top contact layer results in a larger optical bandgap due to the Moss-Burstein effect and is the source of the signal at the shorter wavelength for both structures A and B. It is also important to mention that reverse bias signal is (30–50 times) weaker than

^{a)}Tel.: (505) 272 7800. FAX: (505) 272 7801. Electronic mail: skrishna@chtm.unm.edu

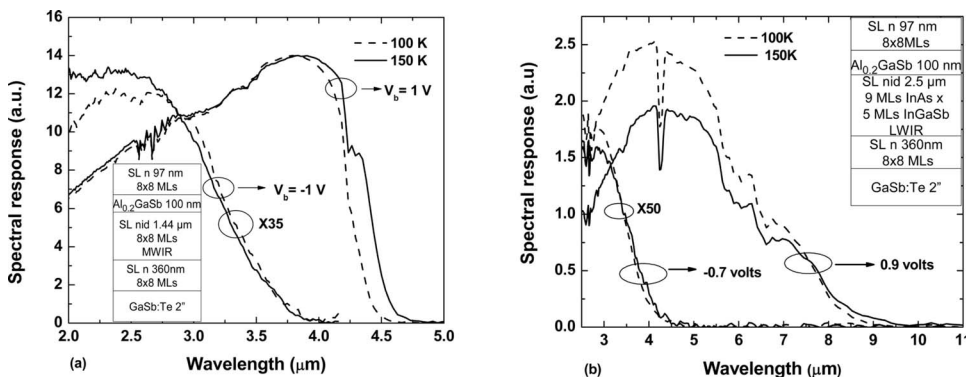


FIG. 1. (a) Spectral response of structure A ($\lambda_{c1} \sim 3.5 \mu\text{m}$ and $\lambda_{c2} \sim 4.5 \mu\text{m}$) at different temperatures under forward and reverse bias; V_b is the applied voltage. The inset shows the schematic of structure A for midwave infrared. (b) Spectral response of structure B ($\lambda_{c1} \sim 3.5 \mu\text{m}$ and $\lambda_{c2} \sim 8 \mu\text{m}$) at different temperatures under forward and reverse bias; V_b is the applied voltage. The inset shows the schematic for structure B for midwave-long wave infrared.

the forward bias signal, which is consistent with the fact that the top contact layer is thinner in comparison with the absorber. Detailed processing and radiometric characterization of structures A and B are discussed elsewhere.¹¹

On the basis of results obtained from structures A and B, we grew and fabricated another nBn device (structure C). Structure C was designed to improve the reverse bias signal and consists of thick MWIR and LWIR absorbers on both sides of the barrier. The MWIR and LWIR absorber layers in structure C are the same as the MWIR absorber in structure A and the LWIR absorber in structure B, respectively. The schematic of structure C is shown as inset to Fig. 3. The growth steps for sample C are as follows: first, a 480 nm bottom contact layer consisting of 8 ML InAs:GaTe ($n = 4 \times 10^{18} \text{ cm}^{-3}$)/8 ML GaSb SLS was grown. Then a 1.8 μm thick LWIR absorber formed by unintentionally doped 9 ML InAs/5 ML $\text{In}_{0.25}\text{Ga}_{0.75}\text{Sb}$ SLS was grown followed by a 1.5 μm thick MWIR absorber composed of 8 ML InAs/8 ML GaSb SLS. A 100 nm $\text{Al}_{0.2}\text{Ga}_{0.8}\text{Sb}$ barrier separated the two absorbers. The structure was capped with $\sim 0.1 \mu\text{m}$ top contact layer consisting of 8 ML InAs:GaTe/8 ML GaSb SLS with the same doping level as the bottom contact layer.

The device was processed to operate at normal incidence as single pixel photodiodes with aperture range of 25–300 μm in diameter using standard optical photolithography technique. Processing was initiated with the formation of ohmic contacts on the n -type top contact layer followed by dry etching the device to the top of the barrier between the two absorbers (etch depth $\sim 1.5 \mu\text{m}$) for the mesa definition. Then the wafer was patterned with the photoresist, and a deep dry etch (etch depth $\sim 2 \mu\text{m}$) to the middle of the bottom n -type contact layer was performed. An ohmic contact was evaporated on the bottom contact layer. Ti (500 Å)/Pt (500 Å)/Au (3000 Å) was used as n -contact metal for both top and bottom contacts.

Current-voltage measurements were performed using a semiconductor parameter analyzer for temperatures ranging from 50 to 300 K. The data show that the current density is higher in the forward bias regime (1.25 A/cm² at +0.5 V, 77 K) as compared to the reverse bias (0.34 A/cm² at

–0.5 V, 77 K). This is expected since the forward bias is dominated by the generation currents from the LWIR absorber while the reverse bias is dominated by the generation currents from the MWIR absorber. The current density in structure C is higher than the current densities found for structures A and B which is due to the larger depth of the first etch ($\sim 1.5 \mu\text{m}$) and, therefore, structure C has larger surface currents as compared to the first etch depth for structures A and B ($\sim 100 \text{ nm}$). The relatively large current density in the three structures can be improved with the optimized composition and thickness of the barrier layer. The relative spectral responses for the bicolor structure is shown in Fig. 3. The data clearly show cutoff wavelengths $\lambda_{c1} \sim 4.5 \mu\text{m}$ and $\lambda_{c2} \sim 8 \mu\text{m}$ under different polarities of applied bias. When forward bias is applied, the carriers from the LW absorber are collected, and when the reverse bias is applied, the carriers from the MW absorber are collected. It is to be noted that there will be barriers between unintentionally doped LWIR layer and the bottom n -contact that can impede the transport.

Since most present day ROIC apply a very small bias voltage, we want to investigate the response close to zero bias. Figure 4 shows values of the spectral response of structure C between 0 and +0.1 V. The data clearly indicate that the response cutoff shifts from MW to LW when the applied bias voltage varies between 0 and +0.1 V. The inset in Fig. 4 presents the intensity study of MWIR, and LWIR ratio versus

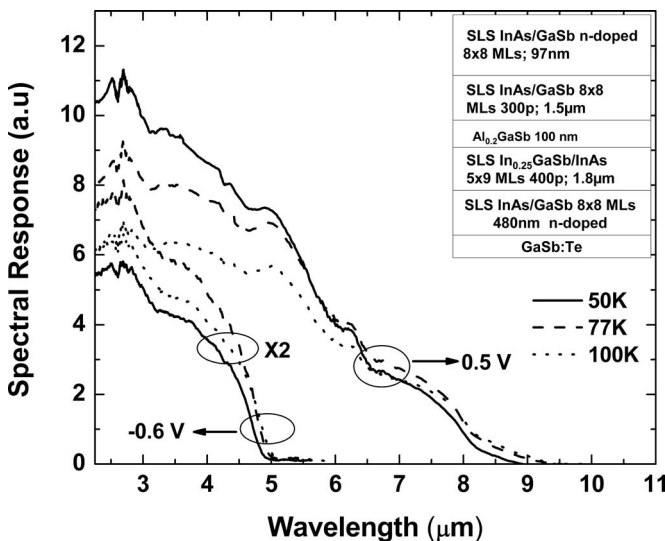


FIG. 3. Spectral response of the bicolor structure at different temperatures under forward and reverse bias; V_b is the applied voltage. The inset shows the structure C for midwave-long wave infrared ($\lambda_{c1} \sim 4.5 \mu\text{m}$ and $\lambda_{c2} \sim 8 \mu\text{m}$).

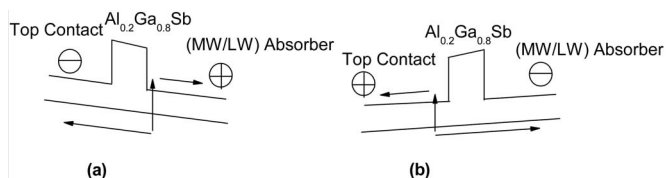


FIG. 2. Conduction band diagram for two color nBn device under (a) forward bias (negative on top) and (b) reverse bias (positive on top).

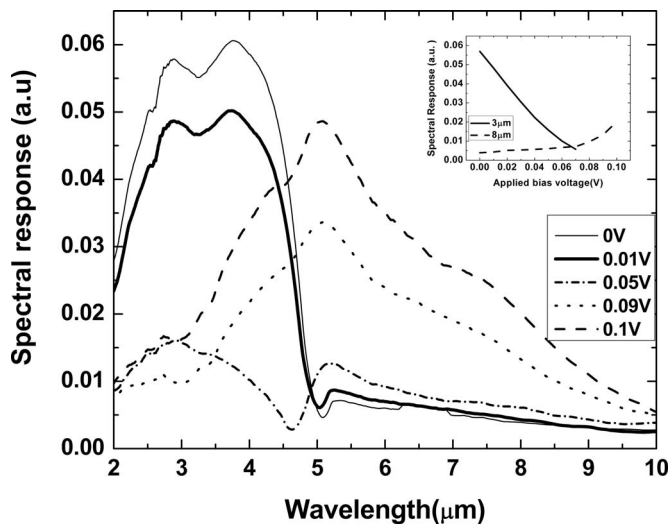


FIG. 4. The spectral response of structure C between 0 and +0.1 V bias voltage, that is, compatible with the bias range of present day ROICs. The inset shows the intensity study of MWIR, and LWIR vs applied bias voltage at 77 K.

applied bias voltage. As the applied bias voltage increases from 0 to +0.1 V, the MW intensity decreases, and LW intensity increases. The bias dependent feature of the spectral response can be exploited by postprocessing algorithms¹² to achieve high levels of spectral tuning and matched filtering. Due to this feature, a single detector can be operated at multiple biases sequentially, whereby the detector's spectral response changes each time with the applied bias. Therefore, the bias dependent spectral response can be used in algorithms to reconstruct the sources in the surrounding environment.

In conclusion, the multispectral capabilities of SLS based nBn structures were demonstrated using three different samples. The SLS devices based on nBn structure exhibited dual band responses in the MW-LW ranges under different bias polarities. A structure was designed to have equal signal strengths from its absorbers under different polarities of applied bias. The spectral response for structure C showed that LW to MW intensity ratio changes within very small bias voltage range which results in less expensive and complex multicolor focal plan array (FPA) technology.

This work is supported by Missile Defense Agency Contract No. HQ0006-05-C-0029.

- ¹A. Rogalski and P. Martyniuk, *Infrared Phys. Technol.* **48**, 39 (2006).
- ²S. Krishna, *Infrared Phys. Technol.* **47**, 1 (2005).
- ³J. B. Rodriguez, E. Plis, S. J. Lee, H. S. Kim, G. Bishop, Y. D. Sharma, L. R. Dawson, and S. Krishna, *Proc. SPIE* **6542**, 654208 (2007).
- ⁴E. Plis, S. Annamalai, K. T. Posani, S. Krishna, R. A. Rupani, and S. Ghosh, *J. Appl. Phys.* **100**, 014510 (2006).
- ⁵Y. Wei, A. Hood, H. Yau, A. Gin, M. Razeghi, M. Z. Tidrow, and V. Nathan, *Appl. Phys. Lett.* **86**, 233106 (2005).
- ⁶S. Maimon and G. W. Wicks, *Appl. Phys. Lett.* **89**, 151109 (2006).
- ⁷J. B. Rodriguez, E. Plis, G. Bishop, Y. D. Sharma, H. S. Kim, L. R. Dawson, and S. Krishna, *Appl. Phys. Lett.* **91**, 043514 (2007).
- ⁸J. F. Scholl, E. L. Dereniak, M. R. Descour, C. P. Tebow, and C. E. Volin, *Appl. Opt.* **42**, 1 (2003).
- ⁹M. Walter, R. Rehm, J. Fleibner, J. Schmitz, J. Ziegler, W. Cabanski, and R. Breiter, *Proc. SPIE* **6542**, 6540206 (2007).
- ¹⁰J. W. Little, S. P. Svensson, W. A. Beck, A. C. Goldberg, S. W. Kennerly, T. Hongmatip, M. Winn, and P. Uppal, *J. Appl. Phys.* **101**, 044514 (2007).
- ¹¹G. Bishop, J. B. Rodriguez, E. Plis, A. Khoshakhlagh, Y. D. Sharma, H. S. Kim, L. R. Dawson, and S. Krishna, *Appl. Phys. Lett.* (submitted).
- ¹²U. Sakoglu, J. Scott, M. Hayat, S. Raghavan, and S. Krishna, *J. Opt. Soc. Am. B* **21**, 1 (2004).